Energies **2014**, *7*, 1750-1769; doi:10.3390/en7031750

OPEN ACCESS

energies

ISSN 1996-1073

www.mdpi.com/journal/energies

Article

H_∞ Fault Tolerant Control of WECS Based on the PWA Model

Yun-Tao Shi *, Qi Kou, De-Hui Sun, Zheng-Xi Li, Shu-Juan Qiao and Yan-Jiao Hou

Key Lab of Field Bus and Automation of Beijing, North China University of Technology, Beijing 100144, China; E-Mails: kouqi0627@gmail.com (Q.K.); sundehui@ncut.edu.cn (D.-H.S.); lzx@ncut.edu.cn (Z.-X.L.); qiaoshujuan001@163.com (S.-J.Q.); houyanjiao0730@163.com (Y.-J.H.)

* Author to whom correspondence should be addressed; E-Mail: shiyuntao@ncut.edu.cn; Tel.: +86-10-8880-2520; Fax: +86-10-8880-3372.

Received: 26 January 2014; in revised form: 13 March 2014 / Accepted: 19 March 2014 / Published: 24 March 2014

Abstract: The main contribution of this paper is the development of H_∞ fault tolerant control for a wind energy conversion system (WECS) based on the stochastic piecewise affine (PWA) model. In this paper the normal and fault stochastic PWA models for WECS including multiple working points at different wind speeds are established. A reliable piecewise linear quadratic regulator state feedback is designed for the fault tolerant actuator and sensor. A sufficient condition for the existence of the passive fault tolerant controller is derived based on some linear matrix inequalities (LMIs). It is shown that the H_∞ fault tolerant controller of WECS can control the wind turbine exposed to multiple simultaneous sensor faults or actuator faults; that is, the reliability of wind turbines can be improved.

Keywords: H_∞ fault tolerant control; piecewise affine; wind energy conversion system; H_∞ robust control

1. Introduction

A wind energy conversion system is a mechanical electronic hydraulic integrated system which consists of rotor, drive train, gear box, generator and other mechanical equipment. WECS driven by stochastic wind power signal indicate nonlinear switching system properties. Control systems play a vital role in satisfying harvested power and load alleviation objectives in wind turbines. The performance of the designed controller can be easily interrupted by possible faults and failures in

different parts of the system. Therefore, designing a fault-tolerant controller is very beneficial in wind turbine operations.

So far, the design of fault-tolerant control for wind turbine systems is still lacking in studies. In [1], Sloth *et al*. presented active and passive fault tolerant controllers for wind turbines. The linear parameter varying control design method is applied which leads to LMI-based optimization in case of active fault tolerant and BLMI in case of passive fault-tolerant problems. In [2], the authors gave the model-based fault detection and control loop reconfiguration for doubly fed induction generators. In [3], generator-converter fault-tolerant control for direct driven wind turbines was investigated. In [4], a fault-tolerant switched reluctance motor was designed for the blade pitch control system.

The above mentioned methods are all restricted to the nonlinear characteristics of wind turbines. In order to overcome the nonlinear characteristics of wind turbines, H_∞ fault tolerant strategy for WECS is proposed in this paper based on a stochastic PWA model framework.

Piecewise linear systems provide a powerful tool of analysis and design for nonlinear control systems. The piecewise linear system framework can be used to analyze smooth nonlinear systems with arbitrary accuracy. Many other classes of nonlinear systems can also be approximated by piecewise linear systems [5].

A number of results have been obtained in controller design of such piecewise continuous time linear systems during the last few years [6–9]. In the case of discrete time, the authors of [10] presented an approach for stabilization of piecewise linear systems based on a global quadratic Lyapunov function. In [5,11], the authors gave a number of results on stability analysis, controller design, H_∞ analysis, and H_∞ controller design for the piecewise linear systems based on a piecewise Lyapunov function. In [5], for H_∞ control synthesis, the affine term was treated as a disturbance. In a recent paper [12], a new method was presented to synthesize the H_∞ controller for the piecewise discrete time linear systems. However, studies solving the fault tolerant control problem of the WECS within the stochastic PWA framework are lacking. In this paper, the stochastic PWA normal, sensor fault and actuator fault models for WECS including multiple work regions are established. A reliable piecewise linear quadratic regulator state feedback is designed such that it can make the actuator and sensor faults tolerant. A sufficient condition for the existence of the passive fault tolerant controller is derived based on some LMIs. The paper is organized as follows: in Section 2, a dynamic model of WECS and the control strategy are briefly described. In Section 3, the normal and fault stochastic PWA models for WECS including multiple working points at different wind speeds are established. H_∞ fault tolerant control for WECS with actuator and sensor faults is also presented. In Section 4, some simulation results are presented. Section 5 gives our conclusions.

2. Literature Review

2.1. Model Structure of WECS

The structure of a WECS is described as Figure 1, in which the WECS inputs are wind speed $v(t)$, pitch angle reference $\beta_{ref}(t)$ and generator torque reference $T_{gref}(t)$, respectively. The outputs of the system are generator power $P_g(t)$ and high-speed shaft speed $\omega_g(t)$.

Figure 1. The structure of WECS.

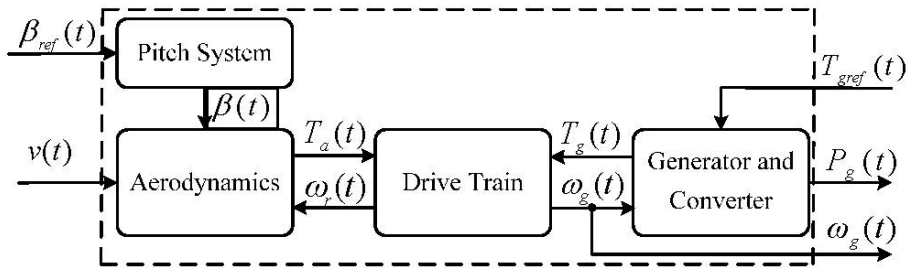

2.2. Wind Model

The equation of wind $v(t)$ is:

$$v(t) = v_s(t) + v_m(t) \tag{1}$$

where $v_m(t)$ is the low-frequency component (describing long term, low-frequency variations), *i.e.*, average wind speed; and $v_s(t)$ is the turbulence component (corresponding to fast, high-frequency variations).

2.3. Aerodynamics Model

The available power in the wind P_w can be expressed as:

$$P_w = \frac{1}{2}\rho A v^3 \tag{2}$$

where A is the rotor swept area; v is the rotor effective wind speed; ρ is the air density, which is assumed to be constant.

From the available power in the wind, the power captured by the rotor P_a is:

$$P_a = P_w C_p(\lambda, \beta) \tag{3}$$

where $C_p(\lambda, \beta)$ is the power coefficient, which depends on the tip-speed ratio λ and the pitch angle β.

The tip-speed ratio λ is defined as the ratio between the tip speed of the blades and the rotor effective wind speed:

$$\lambda = \frac{R\omega_r}{v} \tag{4}$$

where ω_r is the low-speed shaft speed; and R is the blade length.

2.4. Drive Train Model

The drive train model includes a low-speed shaft, a high-speed shaft, a gear box and flexible device. The drive train dynamics function is given:

$$\begin{cases} \dot{\omega}_r = \dfrac{T_r}{J_r} - \dfrac{\omega_r D_s}{J_r} + \dfrac{\omega_g D_s}{J_r N_g} - \dfrac{\delta K_s}{J_r} \\ \dot{\omega}_g = \dfrac{\omega_r D_s}{J_g N_g} - \dfrac{\omega_g D_s}{J_g N_g{}^2} + \dfrac{\delta K_s}{J_g} - \dfrac{T_g}{J_g} \end{cases} \tag{5}$$

where J_r and J_g are the moments of inertia of the low-speed shaft and the high-speed shaft; K_s is the torsion stiffness of the drive train; D_s is the torsion damping coefficient of the drive train; N_g is the gear ratio; δ is the twist of the flexible drive train with $\dot{\delta} = \omega_r - \frac{\omega_g}{N_g}$.

2.5. Pitch System Model

The pitch system can be modeled by a second-order transfer function [13]:

$$\begin{cases} \dot{\beta} = \dot{\beta} \\ \ddot{\beta} = -\omega_n^2 \beta - 2\xi\omega_n \dot{\beta} + \omega_n^2 \beta_{ref} \end{cases} \tag{6}$$

2.6. Generator and Converter Model

The generator and converter dynamics can be modeled by a first-order transfer function:

$$\dot{T}_g = -\frac{1}{\tau_g} T_g + \frac{1}{\tau_g} T_{gref} \tag{7}$$

where τ_g is the time constant.

The real-time power is described by:

$$P_g = \eta_g \omega_g T_g \tag{8}$$

Then, the dynamics of the WECS can be obtained by combining Equations (5)–(7):

$$\begin{bmatrix} \dot{\omega}_r \\ \dot{\omega}_g \\ \dot{\beta} \\ \ddot{\beta} \\ \dot{T}_g \end{bmatrix} = \begin{bmatrix} \frac{T_r}{J_r} - \frac{\omega_r D_s}{J_r} + \frac{\omega_g D_s}{J_r N_g} - \frac{\delta K_s}{J_r} \\ \frac{\omega_r D_s}{J_g N_g} - \frac{\omega_g D_s}{J_g {N_g}^2} + \frac{\delta K_s}{J_g} - \frac{T_g}{J_g} \\ \dot{\beta} \\ -\omega_n^2 \beta - 2\xi\omega_n \dot{\beta} \\ -\frac{1}{\tau_g} T_g \end{bmatrix} + \begin{bmatrix} 0 & 0 \\ 0 & 0 \\ 0 & 0 \\ \omega_n^2 & 0 \\ 0 & \frac{1}{\tau_g} \end{bmatrix} \begin{bmatrix} \beta_{ref} \\ T_{gref} \end{bmatrix} \tag{9}$$

2.7. Control Strategy

The basic control strategy is described as Figure 2. The control requirements for the power and the speed are different in different wind regions. If $v < v_{cut-in}$, the system stops.

Figure 2. The control strategy for wind turbine.

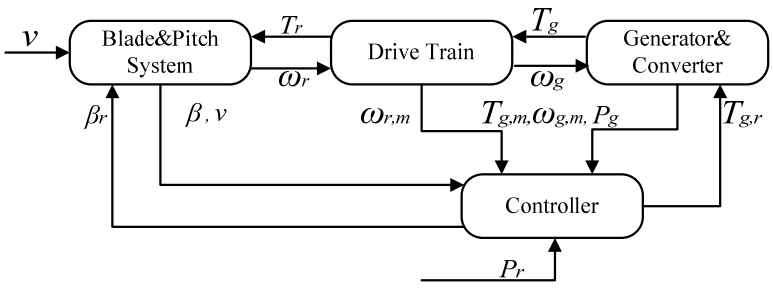

If $v \in [v_{cut-in}, v_{rated}]$, the system needs to maximize the wind harvested power. If $v > v_{rated}$, the system needs to limit power to the rated and maintain the stability of the system.

Figure 3 shows the tendency between the control variables and the controlled variables of the WECS in different workspaces, and the following gives the explanations of each workspace:

A-B: For wind speed under v_{cut-in}, the system stops.

B-C: During the partial load region, the generator control is the only active control and aims at maximizing the energy captured from the wind and/or at limiting the rotational speed at rated. This is possible by continuously accelerating or decelerating the generator speed in such a way that the optimum tip speed ratio is tracked.

C-D: During the full load region, the control objective is to keep the real-time power P_g to the rated value P_{gnom} and limit the high-speed shaft speed ω_g remaining between $[\omega_{gnom}\ \omega_{gmax}]$ at the same time. The main purpose of pitch control is to limit wind capture that is to limit power and avoid the mechanical load increasing.

D-E: When the wind speed is close to $v_{cut-out}$, changing the value of the pitch angle to minimize the wind energy. The system needs to be disconnected from the grid and brake to stop.

Figure 3. The tendency of the β, T_g and P_g following the wind speed.

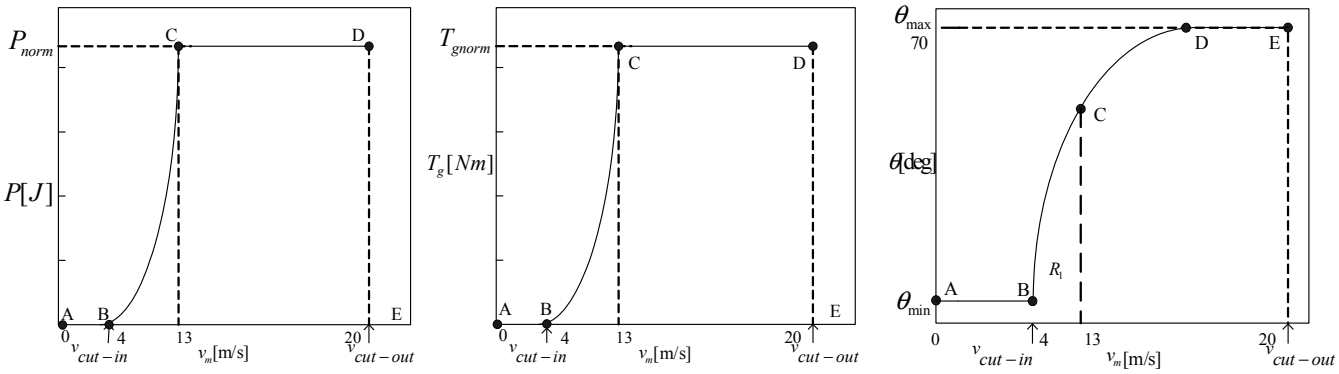

In this paper, we use Maximum Power Point Tracking (MPPT) algorithm to obtain the optimal generator speed ω_{gopt} and the optimal generator power P_{gopt}. The so-called MPPT is a very reliable and robust control method, which covers an entire class of extremum search algorithms to maintain the optimal operating point when the curve $C_p(\lambda, \beta)$ is unknown under a certain wind speed. It can calculate the optimal generator speed ω_{gopt} and the optimal generator power P_{gopt}. The control loop we presented should track the optimal set points of MPPT's outputs.

3. The Proposed Method

3.1. Fault Modelling of WECS within Stochastic PWA Model Framework

In summary, WECS is mainly based on four regions for modeling and control. According to the different wind speeds, models and control strategies need to switch. This section introduces the basic principles of PWA, and then gives the idea of WECS modeling.

3.1.1. Stochastic PWA Model Form

A linear stochastic discrete-time PWA system is defined by the state-space equation:

$$\begin{matrix} x_{k+1} = A_i x_k + B_i u_k + B_i^w w_k + a_i \\ z_k = C_i x_k + D_i u_k + D_i^w w_k \end{matrix}, \quad \begin{bmatrix} x_k \\ u_k \end{bmatrix} \in \chi_i, x_k \in \bar{\chi}_j \tag{10}$$

where $x_k \in \mathbb{R}^n$ is the state; $u_k \in \mathbb{R}^m$ is the control input; $w_k \in \mathbb{R}^r$ is a disturbance signal and $z_k \in \mathbb{R}^m$ is a performance output. The set $\mathbb{X} \subseteq \mathbb{R}^{n+m}$ of every possible vector $[x_k^T \quad u_k^T]^T$ is $\mathbb{R}^{n+m}$ or a polyhedron containing the origin; $\{\chi_i\}_{i=1}^s$ is a polyhedral partition of $\mathbb{X}$ and $a_i \in \mathbb{R}^n$ are constant vectors. Each χ_i is regarded as a cell. For simplicity, assume that the cells are polyhedral defined by matrices F_i^x, F_i^u , f_i^x and f_i^u as follows:

$$\chi_i = \{[x^T \quad u^T]^T \text{ such that } F_i^x x \geq f_i^x \text{ and } F_i^u u \geq f_i^u\} \tag{11}$$

and:

$$\bar{\chi}_i = \{x \text{ such that } F_i^x x \geq f_i^x\} \tag{12}$$

$$S_j = \{i \text{ such that } \exists x, u \text{ with } x \in \bar{\chi}_j, [x^T \quad u^T]^T \in \chi_i\} \tag{13}$$

where S_j is the set of all indices i such that χ_i is a cell containing a vector $[x^T \quad u^T]^T$ with $x \in \bar{\chi}_j$ is satisfied. Denote $I = \{1, \ldots, s\}$, which is the set of indices of the cells χ_i; Denote $\mathcal{J} = \{1, \ldots, t\}$, which is the set of indices of the cells $\bar{\chi}_j$. It is important to see that:

$$\bigcup_{j=1}^{t} S_j = I \tag{14}$$

Furthermore, if cells χ_i have the structure pointed out in Equation (11), then the sets S_j are disjoint. If cells χ_i have a more complicate structure (for instance when mixed state-input constraints are used to define each cell χ_i), then the set S_j could be overlapping.

3.1.2. Stochastic PWA Model for WECS

The linearized drive train dynamics function is described as follows:

$$\begin{cases} \dot{\omega}_r = \dfrac{1}{3J_r}\dfrac{\partial T_a}{\partial \beta}\beta + \dfrac{B_{dt}}{N_g J_r}\omega_g + \left(-\dfrac{B_{dt}+B_r}{J_r} + \dfrac{1}{J_r}\dfrac{\partial T_a}{\partial \omega_r}\right)\omega_r + \dfrac{1}{3J_r}\dfrac{\partial T_a(t)}{\partial v_r}v(t) \\ \dot{\omega}_g = -\dfrac{1}{J_g}T_g - \left(\dfrac{\eta_{dt}B_{dt}}{J_g N_g^2} + \dfrac{B_g}{J_g}\right)\omega_g + \dfrac{B_{dt}}{N_g J_g}\omega_r \end{cases} \tag{15}$$

where $\frac{\partial T_a}{\partial \beta}$、 $\frac{\partial T_a}{\partial \omega_r}$ and $\frac{\partial T_a(t)}{\partial v_r}$ are the linearized parameters in different working points; B_g is the viscous friction of the high speed shaft.

Then a linearized overall state space model describing the dynamics of the WECS can be given:

$$\begin{bmatrix}\dot{T}_g\\ \dot{\beta}\\ \ddot{\beta}\\ \dot{\omega}_g\\ \dot{\omega}_r\end{bmatrix}=\begin{bmatrix}A_{11} & 0 & 0 & 0 & 0\\ 0 & 0 & I & 0 & 0\\ 0 & A_{54} & A_{55} & 0 & 0\\ a_{71} & 0 & 0 & a_{77} & \frac{B_{dt}}{N_gJ_g}\\ 0 & a_{84} & 0 & \frac{B_{dt}}{N_gJ_r} & a_{88}\end{bmatrix}\begin{bmatrix}T_g\\ \beta\\ \dot{\beta}\\ \omega_g\\ \omega_r\end{bmatrix}+\begin{bmatrix}0\\ 0\\ 0\\ 0\\ e_{81}\end{bmatrix}v(t)+\begin{bmatrix}B_{11} & 0\\ 0 & 0\\ 0 & B_{42}\\ 0 & 0\\ 0 & 0\end{bmatrix}\begin{bmatrix}T_{gref}\\ \beta_{ref}\end{bmatrix} \tag{16}$$

where $A_{11}=-\frac{1}{\tau_g}, A_{54}=-\omega_n^2, A_{55}=-2\xi\omega_n, a_{71}=-\frac{1}{J_g}, a_{77}=-\left(\frac{\eta_{dt}B_{dt}}{J_gN_g^2}+\frac{B_g}{J_g}\right), a_{84}=\frac{1}{3J_r}\frac{\partial T_a}{\partial\beta}$, $a_{88}=-\frac{B_{dt}+B_r}{J_r}+\frac{1}{J_r}\frac{\partial T_a}{\partial\omega_r}, B_{11}=\frac{1}{\tau_g}, B_{42}=\omega_n^2, e_{81}=\frac{1}{3J_r}\frac{\partial T_a(t)}{\partial v_r}$.

Although wind can provide the energy that drives the wind turbine, due to its intermittent nature, it also acts as a disturbance. Hence, the effective wind (Equation (1)) can also be considered as a superposition of the mean wind speed v_m, which could be either constant or time varying as a result of a sophisticated forecasting method, and a stochastic component v_s. From [14,15], the stochastic part v_s can be considered as the point wind after a second-order filter, which models the effect of the disc-shaped area swept by the rotor blades. In the frequency domain the power density spectrum S_{v_s} of v_s can be written as $S_{v_s}(f,v_m)=S_p(f)S_f(f,v_m)$, where $S_p(f)$ is the spectrum of the point wind and $S_f(f,v_m)$ denotes the filter, which depends on the mean wind speed. This nonlinear expression can be then approximated by a linear second-order transfer function driven by a white noise process:

$$\begin{cases}\dot{\omega}_1=\omega_2\\ \dot{\omega}_2=-a_1\omega_1+a_2\omega_2+a_3e\end{cases} \tag{17}$$

where $\omega_1=v_s$, $e\in\mathcal{N}(0,1)$; and a_1,a_2,a_3 are parameters depending on the mean wind speed.

Combining with Equation (17), model (16) can be translated into the following form:

$$\begin{bmatrix}\dot{T}_g\\ \dot{\beta}\\ \ddot{\beta}\\ \dot{\omega}_g\\ \dot{\omega}_r\\ \dot{\omega}_1\\ \dot{\omega}_2\end{bmatrix}=\begin{bmatrix}A_{11} & 0 & 0 & 0 & 0 & 0 & 0\\ 0 & 0 & I & 0 & 0 & 0 & 0\\ 0 & A_{54} & A_{55} & 0 & 0 & 0 & 0\\ a_{71} & 0 & 0 & a_{77} & \frac{B_{dt}}{N_gJ_g} & 0 & 0\\ 0 & a_{84} & 0 & \frac{B_{dt}}{N_gJ_r} & a_{88} & 0 & 0\\ 0 & 0 & 0 & 0 & 0 & 0 & 1\\ 0 & 0 & 0 & 0 & 0 & -a_1 & -a_2\end{bmatrix}\begin{bmatrix}T_g\\ \beta\\ \dot{\beta}\\ \omega_g\\ \omega_r\\ \omega_1\\ \omega_2\end{bmatrix}+\begin{bmatrix}B_{11} & 0\\ 0 & 0\\ 0 & B_{42}\\ 0 & 0\\ 0 & 0\\ 0 & 0\\ 0 & 0\end{bmatrix}\begin{bmatrix}T_g^*\\ \beta^*\end{bmatrix}+\begin{bmatrix}0\\ 0\\ 0\\ 0\\ e_{81}\\ 0\\ 0\end{bmatrix}v_m+\begin{bmatrix}0\\ 0\\ 0\\ 0\\ e_{81}\\ 0\\ a_3\end{bmatrix}e \tag{18}$$

Figure 4. Wind speed *vs.* the corresponding working point.

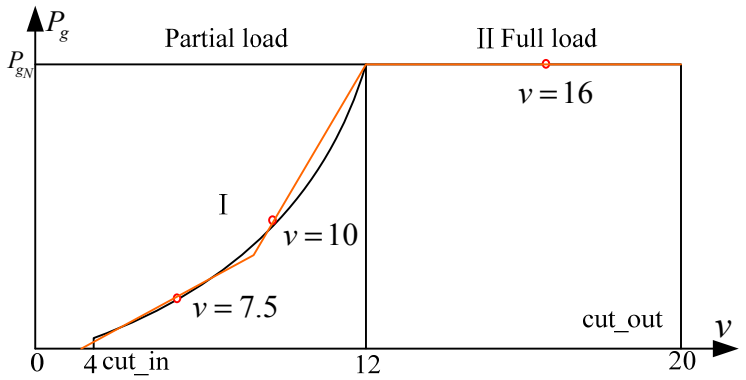

Choose 3 working points for the parameters of WECS described as Figure 4. The values of $\frac{\partial T_a}{\partial \beta}$, $\frac{\partial T_a}{\partial \omega_r}$ and $\frac{\partial T_a(t)}{\partial v_r}$ in different working points can be obtained according to different wind speeds by an effective wind estimator [16], where the realization method is described in [17–20]. The parameters are shown in Tables 1 and 2.

Table 1. Model parameters.

Parameter	Value	Unit	Parameter	Value	Unit
J_r	90,000	$\text{kg} \cdot \text{m}^2$	$P_{g,nom}$	225	kW
J_g	10	$\text{kg} \cdot \text{m}^2$	$\omega_{r,nom}$	4.29	rad/s
K_s	8×10^6	Nm/rad	$\omega_{g,nom}$	105.534	rad/s
D_s	8×10^4	$\text{kg} \cdot \text{m}^2/(\text{rad} \cdot \text{s})$	$\omega_{r,min}$	3.5	rad/s
N_g	24.6	-	$\omega_{g,min}$	86.1	rad/s
$\mathcal{R}$	14.5	m	θ_{min}	0	deg
τ_θ	0.15	s	θ_{max}	25	deg
τ_Γ	0.1	s	$\lvert\dot{\theta}\rvert_{max}$	10	deg/s

Table 2. Parameters of linearized model in different working points.

Wind Speed/ms^{-1}	Parameters					
	a_{84}	a_{88}	e_{81}	a_1	a_2	a_3
$V = 7.5$	0.409	0.50	1.90	0.3125	2.92	0.9375
$V = 10$	0.479	0.53	2.31	0.33	3.65	2.3
$V = 16$	0.833	0.53	2.50	0.625	5	5

3.1.3. WECS Actuator Fault and Sensor Fault Model

In this section, we consider both actuator and sensor faults. Let u_j denote the $j'th$ actuator or sensor, and ${u_j}^F$ denote the failed $j'th$ actuator or sensor. We model a loss of gain in an actuator or sensor as:

$$ {u_j}^F = (1 - \alpha_j)u_j, \quad 0 \le \alpha_j \le \alpha_{Mj} \tag{19} $$

where α_j is the percentage of failure in the j'th actuator or sensor, α_{Mj} is the maximum loss in the j'th actuator or sensor. $\alpha_j = 0$ represents the case without faults in the j'th actuator or sensor, $0 < \alpha_j < 1$ corresponds to the partial loss of the j'th actuator or sensor fault, and $\alpha_j = 1$ corresponds to the all loss of the j'th actuator or sensor fault. Define α with $\alpha = diag\{\alpha_1, \alpha_2, \ldots, \alpha_m\}$. Then $u^F = \Gamma u$, where $\Gamma = (I - \alpha)$. The faults considered are shown in Table 3:

Table 3. The faults considered.

Fault	Type	Fault Description
actuator	gain Factor	Γ_a
sensor	gain Factor	Γ_s

where Γ_a and Γ_s are both diagonal matrix of two elements.

The PWA model of the system with the loss of gain Γ_a in actuators can be described by:

$$ \begin{matrix} x_{k+1} = A_i x_k + B_i \Gamma_a u_k + B_i^w w_k + a_i \\ z_k = C_i x_k + D_i u_k + D_i^w w_k \end{matrix}, \quad \begin{bmatrix} x_k \\ u_k \end{bmatrix} \in \chi_i, x_k \in \bar{\chi}_j \tag{20} $$

and the PWA model of the system with the loss of gain Γ_s in sensors can be described by:

$$\begin{matrix} x_{k+1} = A_i x_k + B_i u_k + B_i^w w_k + a_i \\ z_k = C_i \Gamma_s x_k + D_i u_k + D_i^w w_k \end{matrix}, \quad \begin{bmatrix} x_k \\ u_k \end{bmatrix} \in \chi_i, x_k \in \bar{\chi}_j \tag{21}$$

3.2. H_∞ Fault Tolerant Control for WECS

3.2.1. Fault Tolerant Control for Actuator Fault

Consider the PWA actuator faults system (20), define the input signal w_k as follows:

$$\widetilde{w}_k = \begin{bmatrix} w_k \\ a_i \end{bmatrix} \tag{22}$$

Thus, system (20) can be rewritten as:

$$\begin{matrix} x_{k+1} = A_i x_k + B_i \Gamma_a u_k + \tilde{B}_i^w \widetilde{w}_k \\ z_k = C_i x_k + D_i u_k + \widetilde{D}_i^w \widetilde{w}_k \end{matrix}, \quad \begin{bmatrix} x_k \\ u_k \end{bmatrix} \in \chi_i, x_k \in \bar{\chi}_j \tag{23}$$

where:

$$\tilde{B}_i^w = [B_i^w \quad I], \widetilde{D}_i^w = [D_i^w \quad I] \tag{24}$$

The H_∞ framework considered here is based on a finite horizon definition of the l_2 gain and, consequently, the proposed extension of the disturbance input is sensible [21–24].

Clearly, it is possible to apply the control approach proposed in [5] directly to the extended system (Equation (23)). This can be conservative because a_i is not an unknown disturbance but a known term. Unfortunately, in general, a_i is known only when the control signal u_k has already been calculated. Under the standard assumption:

$$a_i = \bar{a}_j, \forall i \in S_j, \forall j \in \mathcal{J} \tag{25}$$

an alternative control strategy can be proposed. More precisely, the control is assumed to have the following structure:

$$u_k = \begin{bmatrix} K_j^1 & K_j^2 \end{bmatrix} \begin{bmatrix} x_k \\ \bar{a}_j \end{bmatrix}, x_k \in \bar{\chi}_j \tag{26}$$

In this way, the controller can also consider the displacement term $a_i = D\widetilde{w}_k$, where $D = [0 \quad I]$.

By applying the control law (26) to the PWA system (23), we can obtain the closed loop PWA actuator fault system:

$$\begin{matrix} x_{k+1} = \mathcal{A}_{ij} x_k + \tilde{B}_{ij}^w \widetilde{w}_k \\ z_k = \mathcal{C}_{ij} x_k + \widetilde{D}_{ij}^w \widetilde{w}_k \end{matrix}, \quad \begin{bmatrix} x_k \\ u_k \end{bmatrix} \in \chi_i, x_k \in \bar{\chi}_j \tag{27}$$

where:

$$\begin{matrix} \mathcal{A}_{ij} = A_i + B_i \Gamma_a K_j^1, & \tilde{B}_{ij}^w = \tilde{B}_i^w + B_i K_j^2 D \\ \mathcal{C}_{ij} = C_i + D_i K_j^1, & \widetilde{D}_{ij}^w = \widetilde{D}_i^w + D_i K_j^2 D \end{matrix} \tag{28}$$

From the above, we can have the following main results:

Lemma 1. Consider system (27) with zero initial condition $x_0 = 0$, if there exists a function $V(x,u) = x^T P_i x$ for $[x^T \ u^T]^T \in \chi_i$ with $P_i = P_i^T > 0$, satisfying the dissipativity inequality:

$$\forall w \in \mathbb{R}^r, \forall k \geq 0, V(x_{k+1}, \ u_{k+1}) - V(x_k, u_k) < W(z_k, w_k) \tag{29}$$

with supply rate:

$$W_\infty(z,w) = \left(\gamma^2 \|w\|^2 - \|z\|^2\right), \gamma > 0 \tag{30}$$

that is:

$$\forall k, V(x_{k+1}, u_{k+1}) - V(x_k, u_k) < (\gamma^2 \|w_k\|^2 - \|z_k\|^2), \tag{31}$$

then, the H_∞ performance condition:

$$\sum_{\mathrm{k}=0}^{\mathrm{N}} \|z_k\|^2 < \gamma^2 \sum_{k=0}^{N} \|w_k\|^2 \tag{32}$$

is satisfied.

Furthermore, if the following matrix inequalities:

$$\forall j \in \mathcal{J}, , \forall i \in S_j, \forall l \ with \ (l,i) \in S, M_{l,ij} < 0 \tag{33}$$

are satisfied, where:

$$M_{l,ij} = \begin{bmatrix} A_{ij}^T P_i A_{ij} - P_j + C_{ij}^T C_{ij} & C_{ij}^T D_j^w + A_{ij}^T P_i B_j^w \\ D_j^{wT} C_{ij} + B_j^{wT} P_i A_{ij} & B_j^{wT} P_i B_j^w + D_j^{wT} D_j^w - \gamma^2 I \end{bmatrix} \tag{34}$$

then, condition (31) is fulfilled. Thus, system (27) is PWQ stable.

Proof. By recalling that $x_0 = 0$, from Equation (31) it follows that, $\forall N \geq 0$:

$$V(x_{N+1}, u_{N+1}) < \sum_{k=0}^{N} (\gamma^2 \|w_k\|^2 - \|z_k\|^2) \tag{35}$$

Since $V(x_{N+1}, u_{N+1}) > 0$, then condition:

$$\sum_{k=0}^{N} \|z_k\|^2 < \gamma^2 \sum_{k=0}^{N} \|w_k\|^2 \tag{36}$$

is met.

Moreover, if $[x_k^T \quad u_k^T]^T \in \mathcal{X}_i$ and $[x_{k+1}^T \quad u_{k+1}^T]^T \in \mathcal{X}_l$, then:

$$\forall w_k, [x_k^T \ w_k^T] \, M_{l,ij} \, [x_k^T \ w_k^T]^T < 0 \tag{37}$$

Obviously, if condition (33) holds, inequality (37) is satisfied and $\mathcal{C}_{ij}^T \mathcal{C}_{ij} > 0$. For $A_{ij}^T P_l A_{ij} - P_i + C_{ij}^T C_{ij}$, we can state that:

$$\forall j \in \mathcal{J}, \forall i \in S_j, \forall l \ with (l,i) \in S, \mathcal{A}_{ij}^T P_i \mathcal{A}_{ij} - P_i < 0 \tag{38}$$

This implies that system (27) is PWQ stable.

Now we focus on the possibility of finding a state-feedback control law of the type (26) for system (23). The main result is summarized in the following theorem.

Theorem 1. For PWA system (20), there exists a state feedback control law of type (26), which can guarantee PWQ Lyapunov stability and fulfil the dissipativity constraint:

$$\forall w \in \mathbb{R}^r, \forall k \geq 0, V(x_{k+1}) - V(x_k, u_k) < W(z_k, w_k) \tag{39}$$

with supply rate:

$$\widetilde{W}_\infty(z_k, w_k) = (\gamma^2 \left\| [w_k^T \; a_i^T]^T \right\|^2 - \|z_k\|^2) = (\gamma^2 \|(w_k\|^2 + \|a_i\|^2) - \|z_k\|^2), \gamma > 0, \begin{bmatrix} x_k \\ u_k \end{bmatrix} \in \chi_i \tag{40}$$

If there exist matrices $Q_i = Q_i^T > 0$ with $i \in I$ and matrices G_j, Y_j, K_j^2 with $j \in \mathcal{J}$, such that $\forall j \in \mathcal{J}, \forall i \in S_j, \forall l$ with $(l, i) \in S_{all}$:

$$\begin{bmatrix} Q_i - G_j - G_j^T & \left(A_i G_j + B_i \Gamma_a Y_j\right)^T & \left(C_i G_j + D_i Y_j\right)^T & 0 \\ A_i G_j + B_i \Gamma_a Y_j & -Q_l & 0 & \tilde{B}_i^w + B_i \Gamma_a K_j^2 D \\ C_i G_j + D_i Y_j & 0 & -I & \tilde{D}_i^w + D_i K_j^2 D \\ 0 & (\tilde{B}_i^w + B_i \Gamma_a K_j^2 D)^T & (\tilde{D}_i^w + D_i K_j^2 D)^T & -\gamma^2 I \end{bmatrix} < 0 \tag{41}$$

holds, then the feedback gains matrices K_j^1 with $j \in \mathcal{J}$ are given by:

$$K_j^1 = Y_j G_j^{-1}. \tag{42}$$

Proof: Using Schur's lemma, then Equation (33) can be rewritten as follows:

$$\begin{bmatrix} -P_i & \left(A_i + B_i \Gamma_a K_j^1\right)^T & \left(C_i + D_i K_j^1\right)^T & 0 \\ A_i + B_i \Gamma_a K_j^1 & P_l^{-1} & 0 & \tilde{B}_i^w + B_i \Gamma_a K_j^2 D \\ C_i + D_i K_j^1 & 0 & -I & \tilde{D}_i^w + D_i K_j^2 D \\ 0 & (\tilde{B}_i^w + B_i \Gamma_a K_j^2 D)^T & (\tilde{D}_i^w + D_i K_j^2 D)^T & -\gamma^2 I \end{bmatrix} < 0 \tag{43}$$

where $A_{ij} = A_i + B_i \Gamma_a K_j^1, C_{ij} = C_i + D_i K_j^1$.

Now, let $Q_l = P_l^{-1}$ and $Y_j = K_j^1 G_j$, we can obtain inequality (41) by multiplying (43) from the left by diag$\left(G_j^T \; I \; I \; I\right)$ and the right by diag$(G_j \; I \; I \; I)$:

Let:

$$H = \begin{bmatrix} G_j^T & 0 & 0 & 0 \\ 0 & I & 0 & 0 \\ 0 & 0 & I & 0 \\ 0 & 0 & 0 & I \end{bmatrix} \tag{44}$$

then:

$$
\begin{aligned}
&H*\begin{bmatrix} -P_i & \left(A_i+B_i\Gamma_a K_j^1\right)^T & \left(C_i+D_iK_j^1\right)^T & 0 \\ A_i+B_i\Gamma_a K_j^1 & -P_l^{-1} & 0 & \tilde{B}_i^w+B_i\Gamma_a K_j^2 D \\ C_i+D_iK_j^1 & 0 & -I & \tilde{D}_i^w+D_iK_j^2 D \\ 0 & (\tilde{B}_i^w+B_i\Gamma_a K_j^2 D)^T & (\tilde{D}_i^w+D_iK_j^2 D)^T & -\gamma^2 I \end{bmatrix}*H^T \\
&=\begin{bmatrix} -G_j^T P_i G_j & G_j^T\left(A_i+B_i\Gamma_a K_j^1\right)^T & G_j^T\left(C_i+D_iK_j^1\right)^T & 0 \\ \left(A_i+B_i\Gamma_a K_j^1\right)G_j & -P_l^{-1} & 0 & \tilde{B}_i^w+B_i\Gamma_a K_j^2 D \\ \left(C_i+D_iK_j^1\right)G_j & 0 & -I & \tilde{D}_i^w+D_iK_j^2 D \\ 0 & (\tilde{B}_i^w+B_i\Gamma_a K_j^2 D)^T & (\tilde{D}_i^w+D_iK_j^2 D)^T & -\gamma^2 I \end{bmatrix} \\
&=\begin{bmatrix} -G_j^T P_i G_j & \left(A_iG_j+B_i\Gamma_a Y_j\right)^T & \left(C_iG_j+D_iY_j\right)^T & 0 \\ A_iG_j+B_i\Gamma_a Y_j & -Q_l & 0 & \tilde{B}_i^w+B_i\Gamma_a K_j^2 D \\ C_iG_j+D_iY_j & 0 & -I & \tilde{D}_i^w+D_iK_j^2 D \\ 0 & (\tilde{B}_i^w+B_i\Gamma_a K_j^2 D)^T & (\tilde{D}_i^w+D_iK_j^2 D)^T & -\gamma^2 I \end{bmatrix}<0
\end{aligned} \tag{45}
$$

Since $0 < G_j + G_j^T - Q_i \le G_j^T Q_i^{-1} G_j$, Equation (45) implies:

$$
\begin{bmatrix} Q_i-G_j-G_j^T & \left(A_iG_j+B_i\Gamma_a Y_j\right)^T & \left(C_iG_j+D_iY_j\right)^T & 0 \\ A_iG_j+B_i\Gamma_a Y_j & -Q_l & 0 & \tilde{B}_i^w+B_i\Gamma_a K_j^2 D \\ C_iG_j+D_iY_j & 0 & -I & \tilde{D}_i^w+D_iK_j^2 D \\ 0 & (\tilde{B}_i^w+B_i\Gamma_a K_j^2 D)^T & (\tilde{D}_i^w+D_iK_j^2 D)^T & -\gamma^2 I \end{bmatrix}<0 \tag{46}
$$

It is obvious to get $Q_i > 0, \forall i \in I$, then the control matrixes K_j^l can be reconstructed as $K_j^1 = Y_j G_j^{-1}$.

3.2.2. Fault Tolerant Control for Sensor Fault

Theorem 2. For PWA system (21), there exists a state feedback control law of type (26), which can guarantee PWQ Lyapunov stability and fulfil the dissipativity constraint:

$$\forall w \in \mathbb{R}^r, \forall k \ge 0, V(x_{k+1}) - V(x_k, u_k) < W(z_k, w_k) \tag{47}$$

with supply rate:

$$\widetilde{W}_\infty(z_k, w_k) = (\gamma^2 \left\| [w_k^T \; a_i^T]^T \right\|^2 - \|z_k\|^2) = (\gamma^2 \|(w_k\|^2 + \|a_i\|^2) - \|z_k\|^2), \gamma > 0, \begin{bmatrix} x_k \\ u_k \end{bmatrix} \in \chi_i \tag{48}$$

If there exist matrices $Q_i = Q_i^T > 0$ with $i \in I$ and matrices G_j, Y_j, K_j^2 with $j \in \mathcal{J}$, such that $\forall j \in \mathcal{J}, \forall i \in S_j, \forall l$ with $(l, i) \in S_{all}$:

$$
\begin{bmatrix} Q_i - G_j - G_j^T & (A_iG_j + B_iY_j)^T & (C_i\Gamma_s G_j + D_iY_j)^T & 0 \\ A_iG_j + B_iY_j & -Q_l & 0 & \tilde{B}_i^w + B_iK_j^2 D \\ C_i\Gamma_s G_j + D_iY_j & 0 & -I & \tilde{D}_i^w + D_iK_j^2 D \\ 0 & (\tilde{B}_i^w + B_iK_j^2 D)^T & (\tilde{D}_i^w + D_iK_j^2 D)^T & -\gamma^2 I \end{bmatrix} < 0 \tag{49}
$$

holds, then the feedback gains matrices K_j^l with $j \in \mathcal{J}$ are given by:

$$K_j^1 = Y_j G_j^{-1} \tag{50}$$

Proof: Similar to the proof of Theorem 1, Equation (33) can be rewritten as follows:

$$\begin{bmatrix} -P_i & \left(A_i + B_i K_j^1\right)^T & \left(C_i\Gamma_s + D_i K_j^1\right)^T & 0 \\ A_i + B_i K_j^1 & -P_l^{-1} & 0 & \tilde{B}_i^w + B_i K_j^2 D \\ C_i\Gamma_s + D_i K_j^1 & 0 & -I & \tilde{D}_i^w + D_i K_j^2 D \\ 0 & (\tilde{B}_i^w + B_i K_j^2 D)^T & (\tilde{D}_i^w + D_i K_j^2 D)^T & -\gamma^2 I \end{bmatrix} < 0 \tag{51}$$

where $A_{ij} = A_i + B_i K_j^1, C_{ij} = C_i\Gamma_s + D_i K_j^1$.

Now, let $Q_l = P_l^{-1}$ and $Y_j = K_j^1 G_j$, we can also obtain inequality (49) by multiplying (51) from the left by diag$\left(G_j^T\ I\ I\ I\right)$ and the right by diag$(G_j\ I\ I\ I)$.The rest proof process is similar to Theorem 1, omitted here.

4. Simulation Results

According to the modeling method described in part 3, we can obtain the following PWA model of WECS:

If $0 < E_1 x_k \leq 8$ (Region 1), then:

$$\begin{bmatrix} \dot{T}_g \\ \dot{\beta} \\ \ddot{\beta} \\ \dot{\omega}_g \\ \dot{\omega}_r \\ \dot{w}_1 \\ \dot{w}_2 \end{bmatrix} = \begin{bmatrix} -10 & 0 & 0 & 0 & 0 & 0 & 0 \\ 0 & 0 & 1 & 0 & 0 & 0 & 0 \\ 0 & -123.4 & -13.332 & 0 & 0 & 0 & 0 \\ -0.1 & 0 & 0 & -13.2 & 325.2 & 0 & 0 \\ 0 & -0.409 & 0 & 0.036 & -0.5 & 0 & 0 \\ 0 & 0 & 0 & 0 & 0 & 0 & 1 \\ 0 & 0 & 0 & 0 & 0 & -0.3125 & -2.92 \end{bmatrix} \begin{bmatrix} T_g \\ \beta \\ \dot{\beta} \\ \omega_g \\ \omega_r \\ \omega_1 \\ \omega_2 \end{bmatrix} + \begin{bmatrix} 10 & 0 \\ 0 & 0 \\ 0 & 123.4 \\ 0 & 0 \\ 0 & 0 \\ 0 & 0 \\ 0 & 0 \end{bmatrix} \begin{bmatrix} T_{gref} \\ \beta_{ref} \end{bmatrix} + \begin{bmatrix} 0 \\ 0 \\ 0 \\ 0 \\ 1.9 \\ 0 \\ 0 \end{bmatrix} \times 7.5 + \begin{bmatrix} 0 \\ 0 \\ 0 \\ 0 \\ 1.9 \\ 0 \\ 0.9325 \end{bmatrix} e \tag{52}$$

If $8 < E_1 x_k \leq 12$ (Region 2), then:

$$\begin{bmatrix} \dot{T}_g \\ \dot{\beta} \\ \ddot{\beta} \\ \dot{\omega}_g \\ \dot{\omega}_r \\ \dot{w}_1 \\ \dot{w}_2 \end{bmatrix} = \begin{bmatrix} -10 & 0 & 0 & 0 & 0 & 0 & 0 \\ 0 & 0 & 1 & 0 & 0 & 0 & 0 \\ 0 & -123.4 & -13.332 & 0 & 0 & 0 & 0 \\ -0.1 & 0 & 0 & -13.2 & 325.2 & 0 & 0 \\ 0 & -0.479 & 0 & 0.036 & -0.53 & 0 & 0 \\ 0 & 0 & 0 & 0 & 0 & 0 & 1 \\ 0 & 0 & 0 & 0 & 0 & -0.33 & -3.65 \end{bmatrix} \begin{bmatrix} T_g \\ \beta \\ \dot{\beta} \\ \omega_g \\ \omega_r \\ \omega_1 \\ \omega_2 \end{bmatrix} + \begin{bmatrix} 10 & 0 \\ 0 & 0 \\ 0 & 123.4 \\ 0 & 0 \\ 0 & 0 \\ 0 & 0 \\ 0 & 0 \end{bmatrix} \begin{bmatrix} T_{gref} \\ \beta_{ref} \end{bmatrix} + \begin{bmatrix} 0 \\ 0 \\ 0 \\ 0 \\ 2.31 \\ 0 \\ 0 \end{bmatrix} \times 10 + \begin{bmatrix} 0 \\ 0 \\ 0 \\ 0 \\ 2.31 \\ 0 \\ 2.3 \end{bmatrix} e \tag{53}$$

If $12 < E_1 x_k \leq 18$ (Region 3), then:

$$\begin{bmatrix} \dot{T}_g \\ \dot{\beta} \\ \ddot{\beta} \\ \dot{\omega}_g \\ \dot{\omega}_r \\ \dot{w}_1 \\ \dot{w}_2 \end{bmatrix} = \begin{bmatrix} -10 & 0 & 0 & 0 & 0 & 0 & 0 \\ 0 & 0 & 1 & 0 & 0 & 0 & 0 \\ 0 & -123.4 & -13.332 & 0 & 0 & 0 & 0 \\ -0.1 & 0 & 0 & -13.2 & 325.2 & 0 & 0 \\ 0 & -0.833 & 0 & 0.036 & -0.53 & 0 & 0 \\ 0 & 0 & 0 & 0 & 0 & 0 & 1 \\ 0 & 0 & 0 & 0 & 0 & -0.625 & -5 \end{bmatrix} \begin{bmatrix} T_g \\ \beta \\ \dot{\beta} \\ \omega_g \\ \omega_r \\ \omega_1 \\ \omega_2 \end{bmatrix} + \begin{bmatrix} 10 & 0 \\ 0 & 0 \\ 0 & 123.4 \\ 0 & 0 \\ 0 & 0 \\ 0 & 0 \\ 0 & 0 \end{bmatrix} \begin{bmatrix} T_{gref} \\ \beta_{ref} \end{bmatrix} + \begin{bmatrix} 0 \\ 0 \\ 0 \\ 0 \\ 2.5 \\ 0 \\ 0 \end{bmatrix} \times 16 + \begin{bmatrix} 0 \\ 0 \\ 0 \\ 0 \\ 2.5 \\ 0 \\ 5 \end{bmatrix} e \tag{54}$$

where $E_1 = [0\ 0\ 0\ 0\ 0\ 1\ 0]$.

According to Theorem 1 and Theorem 2, we can successfully obtain the piecewise linear state feedback matrixes K_1, K_2, K_3 of WECS system in normal, sensor failure and actuator failure cases. The feedback matrixes calculated in the three cases are shown as follows:

The normal WECS:

$$K_1 = \begin{bmatrix} -0.0859 & -0.0149 & -0.0009 & 0.0018 & 0.2721 & 0.0000 & 0.0000 & -0.0066 & -0.0247 \\ -0.0334 & -0.1671 & -0.0121 & 0.0080 & 2.4130 & 0.0000 & 0.0000 & -0.0130 & 0.0000 \end{bmatrix} \quad (55)$$

$$K_2 = \begin{bmatrix} 7.6202 & -0.7650 & -0.0482 & 0.0031 & 0.1483 & 0.0000 & 0.0000 & -0.4561 & -0.8690 \\ 81.4923 & -24.3547 & -1.6292 & 1.4002 & 396.2525 & 0.0000 & 0.0000 & -17.8043 & -0.0099 \end{bmatrix} \quad (56)$$

$$K_3 = \begin{bmatrix} 0.3367 & -0.0142 & -0.0009 & -0.0024 & 0.2854 & 0.0000 & 0.0000 & -0.0055 & -0.0142 \\ 3.9585 & -0.1744 & -0.0186 & -0.0379 & 3.7296 & 0.0000 & 0.0000 & -0.0441 & 0.0000 \end{bmatrix} \quad (57)$$

Actuator within fault tolerance:

$$K_1 = \begin{bmatrix} -0.1431 & -0.0248 & -0.0015 & 0.0030 & 0.4536 & 0.0000 & 0.0000 & -0.0110 & -0.0411 \\ -0.0556 & -0.2784 & -0.0201 & 0.0134 & 4.0216 & 0.0000 & 0.0000 & -0.0217 & 0.0000 \end{bmatrix} \quad (58)$$

$$K_2 = \begin{bmatrix} 12.7003 & -1.2750 & -0.0804 & 0.0052 & 24.4886 & 0.0000 & 0.0000 & -0.7601 & -1.4483 \\ 135.8205 & -40.5912 & -2.7154 & 2.3337 & 660.4208 & 0.0000 & 0.0000 & -29.6738 & -0.0166 \end{bmatrix} \quad (59)$$

$$K_3 = \begin{bmatrix} 0.1833 & -0.0077 & -0.0005 & -0.0013 & 0.1554 & 0.0000 & 0.0000 & -0.0030 & -0.0078 \\ 2.1305 & -0.0967 & -0.0102 & -0.0202 & 2.0492 & 0.0000 & 0.0000 & 0.0222 & 0.0000 \end{bmatrix} \quad (60)$$

Sensor within fault tolerance:

$$K_1 = \begin{bmatrix} -0.1110 & -0.0138 & -0.0009 & 0.0019 & 0.2541 & 0.0000 & 0.0000 & -0.0053 & -0.0247 \\ 0.0000 & -0.1721 & -0.0124 & 0.0079 & 2.4826 & 0.0000 & 0.0000 & -0.0184 & 0.0000 \end{bmatrix} \quad (61)$$

$$K_2 = \begin{bmatrix} -0.1652 & -0.0208 & -0.0013 & 0.0030 & 0.3894 & 0.0000 & 0.0000 & -0.0086 & -0.0363 \\ 0.0000 & -0.2548 & -0.0183 & 0.0119 & 3.7666 & 0.0000 & 0.0000 & -0.0269 & 0.0000 \end{bmatrix} \quad (62)$$

$$K_3 = \begin{bmatrix} -0.1682 & -0.0210 & -0.0013 & 0.0030 & 0.3930 & 0.0000 & 0.0000 & -0.0085 & -0.0377 \\ -0.0008 & -0.2175 & -0.0159 & 0.0062 & 2.9796 & 0.0000 & 0.0000 & 0.0228 & 0.0001 \end{bmatrix} \quad (63)$$

In these three cases, feedback gains K_1, K_2, K_3 correspond to Regions 1, 2, 3, respectively. The feedback gains K_1, K_2, K_3 are designed according to the stochastic PWA model of WECS. When the model switches, corresponding the feedback gain switches. Then the piecewise linear state feedbacks can guarantee the WECS systems meeting PWQ Lyapunov stability.

4.1. Validation of H_∞ Control for the Normal WECS

Figure 5 demonstrates the simulation results of WECS fault free dynamic response which is regulated by the robust H_∞ controller designed based on Theorem 1. Figure 5a is the test wind speed signal which is consisted of mean wind speed v_m and wind speed turbulent v_s ($v = v_m + v_s$). $v_m = 7.5,\ 10,\ 16\ (m/s),$ which is switched at time of 100 s, 200 s, 300 s, respectively. The tip speed ratio and the optimal generator power set point calculated by MPPT algorithm are given by Figure 5b,c,

respectively, which are under the control of reliable H_∞ controller designed based on the stochastic PWA model of WECS.

Figure 5. H_∞ reliable control for normal WECS based on stochastic PWA model: (**a**) wind speed (m/s); (**b**) tip speed ratio; (**c**) optimal ω_g setpiont (rad/s); (**d**) generator speed (rad/s); (**e**) generator power (KW); (**f**) pitch angle (°); (**g**) generator torque (Nm).

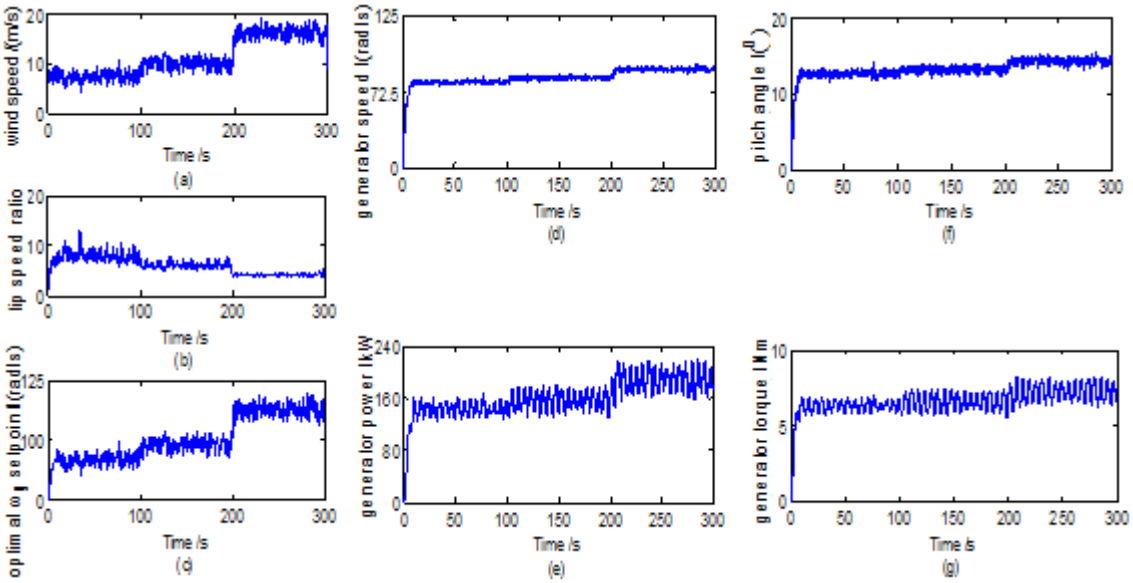

The generator speed and generator power responses are shown in Figure 5d,e, from which we can conclude the real generator power tracks the optimal set point quite well and the generator speed is controlled with good performance. Figure 5f,g give the H_∞ controller output of pitch angle β and generator torque T_g. Figure 5 show the H_∞ controller of WECS designed based on stochastic PWA model combining with MPPT module works quite well.

4.2. Validation of H_∞ Control for WECS with Actuators Fault

Figure 6a–c show that with the pitch system actuator gain fault β_f and the generator gain fault T_{gf} (let gain loss factor $\Gamma_a = \begin{bmatrix} 0.6 & 0 \\ 0 & 0.6 \end{bmatrix}$), the MPPT module works quite well. Comparing with Figure 5a–c, there are little changes.

However, comparing with Figure 5d,e, the performance of generator power P_{gf} and generator speed ω_{gf} have deteriorated, and begin to show the trend of losing stability. The control variables display wide range oscillations in Figure 6f,g. It is seen that the normal H_∞ controller for WECS cannot deal with the actuators fault with gain factor loss Γ_a. Comparing Figure 6d,e, Figure 7d,e demonstrate the response of generator speed and generator power under the control of H_∞ fault tolerant controller designed based on Theorem1 based on the stochastic PWA actuator fault model of WECS, from which we can see that the performance with fault tolerant design significantly is better than the normal controller.

Figure 6. Actuators fault of WECS without fault tolerant control: (**a**) wind speed (m/s); (**b**) the tip speed ratio; (**c**) optimal ω_g setpiont (rad/s); (**d**) generator speed (rad/s); (**e**) generator power (KW); (**f**) the pitch angle (°); (**g**) the generator torque (Nm).

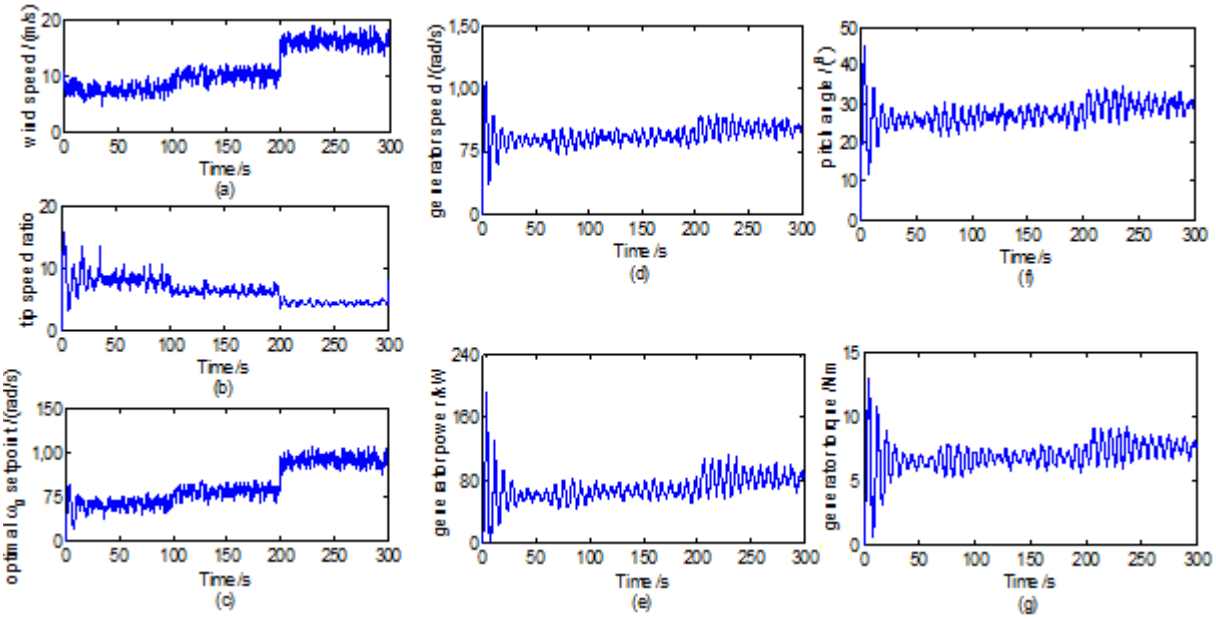

Figure 7. H_∞ fault tolerant control for actuators fault of WECS: (**a**) wind speed (m/s); (**b**) tip speed ratio; (**c**) optimal ω_g setpiont (rad/s); (**d**) generator speed (rad/s); (**e**) generator power (KW); (**f**) pitch angle (°); (**g**) generator torque (Nm).

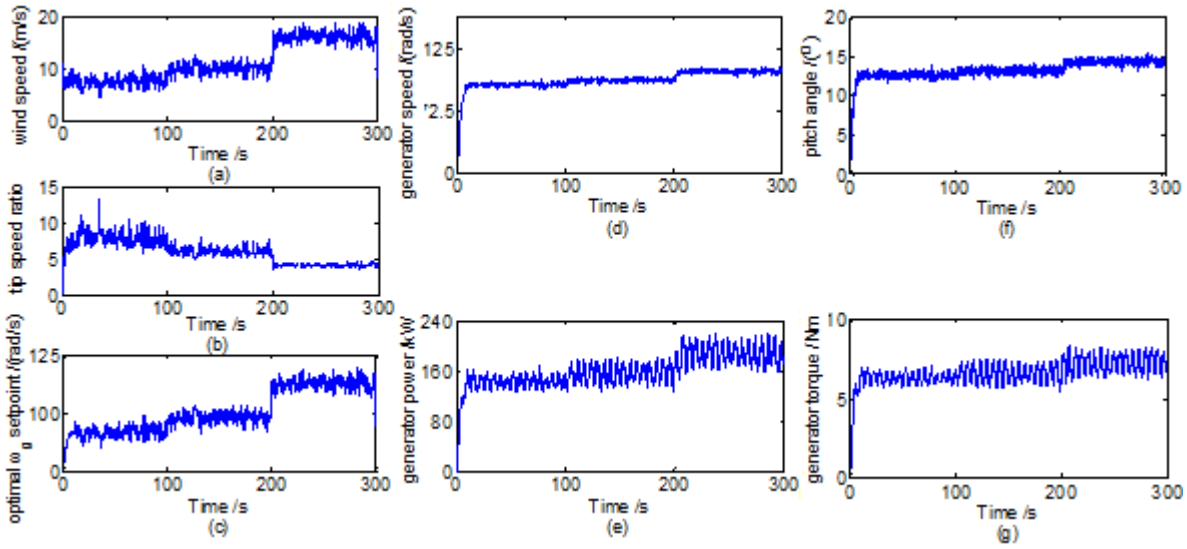

4.3. Validation of H_∞ Control for WECS with Sensors Fault

Figures 8 and 9 demonstrate the simulation results of WECS with sensor gain factor fault (let gain loss factor $\Gamma_s = \begin{bmatrix} 1.2 & 0 \\ 0 & 1.2 \end{bmatrix}$) including generator speed sensor fault w_{gf} and generator power sensor fault p_{gf}. In Figure 8, the dynamic behaviors of WECS under the normal controller without fault tolerant design for two sensor fault are demonstrated. In Figure 9 the H_∞ fault tolerant controller is synthesized

based on the stochastic PWA model of WECS with sensor fault using the Theorem 2. In Figure 8d,e, the performances of generator power P_{gf} and generator speed W_{gf} have deteriorated and totally lose stability. The control variables which are shown in Figure 8e,f display wide range oscillations. While in Figure 9e,f, with the help of fault tolerant controller, the outputs of WECS with sensor faults can obtain better performance than the normal controller. But the generator power and generator speed cannot track the optimal set point of MPPT module's output. This problem should be further investigated.

Figure 8. Sensors fault of WECS without fault tolerant control: (**a**) wind speed (m/s); (**b**) tip speed ratio; (**c**) optimal ω_g setpiont (rad/s); (**d**) generator speed (rad/s); (**e**) generator power (KW); (**f**) pitch angle (°); (**g**) generator torque (Nm).

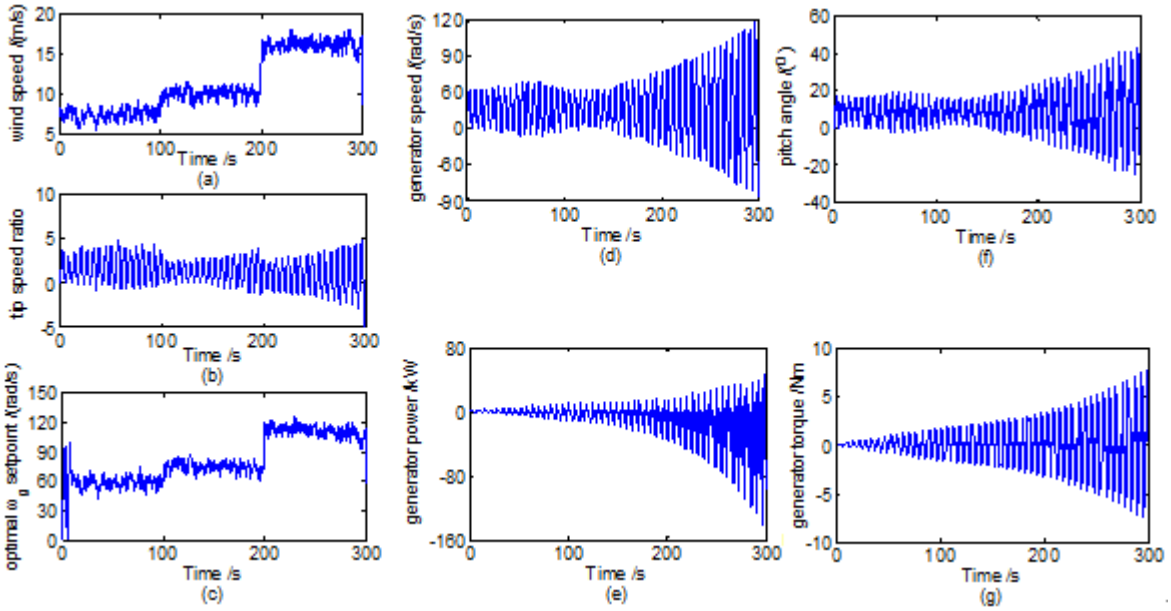

Figure 9. H_∞ fault tolerant control for sensors fault of WECS: (**a**) wind speed (m/s); (**b**) tip speed ratio; (**c**) optimal ω_g set point (rad/s); (**d**) generator speed (rad/s); (**e**) generator power (KW); (**f**) pitch angle (°); (**g**) generator torque (Nm).

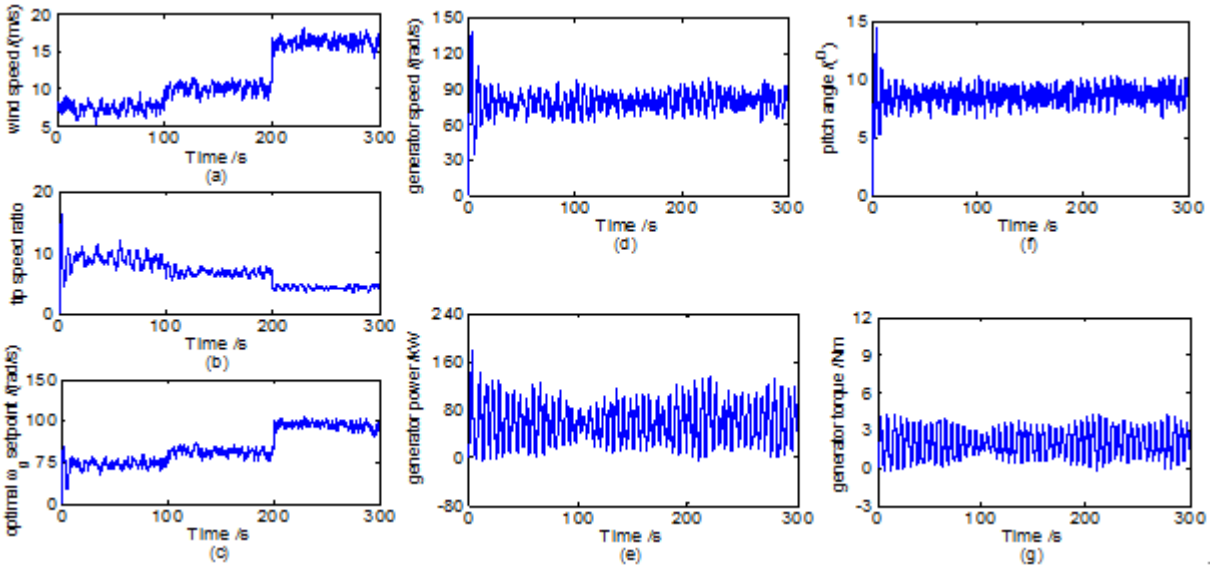

5. Conclusions

From the discussion in Section 3, it is shown that the stochastic PWA model offers an ideal framework for capturing the stochastic property of wind speed and the nonlinear dynamics of WECS. The pictures that emerge from the proposed method and simulation results in Sections 3 and 4, suggest that the presented H_∞ fault tolerant control method offers an effective tool to deal with synthesis problem of WECS with sensors and actuator faults. However, the control strategies presented in this paper are mainly investigated for the overall model of WECS which overlooks the nonlinear and high-order dynamic properties of generator and converter. Future research will focus on developing an inner loop vector controller for generator torque control to deal with the nonlinear and high-order generator model. So far, we only finished the simulation work for this paper. We have developed a laboratory setup of a 10 KW WECS simulator which would provide a benchmark for further experimental investigation of the WECS control algorithm we presented in the paper.

Acknowledgments

This work was simultaneously supported by the National Natural Science Foundation of China under Grant No. 61304049, No.61174116, and the Beijing Natural Science Foundation Program 4132021.

Author Contributions

Yuntao Shi designed the simulations and the study, Shujuan Qiao contributed to the derivation of Theorem 1 for actuator fault tolerant control of WECS, and Yanjiao Hou contributed to the derivation of Theorem 2 for sensor fault tolerant control of WECS. All authors performed the simulations, carried out data analysis, discussed the results and contributed to writing the paper.

Conflicts of Interest

The authors declare no conflict of interest.

References

1. Sloth, C.; Esbensen, T.; Stoustrup, J. Active and Passive Fault-Tolerant LPV Control of Wind Turbines. In Proceedings of the 2010 American Control Conference, Baltimore, MD, USA, 30 June 2010–2 July 2010; pp. 4640–4646.
2. Rothenhagen, K.; Fuchs, F.W. Doubly fed induction generator model-based sensor fault detection and control loop reconfiguration. *IEEE Trans. Ind. Electron.* **2009**, *56*, 4229–4238.
3. Parker, M.A.; Ran, L.; Finney, S.J. Distributed control of a fault-tolerant modular multilevel inverter for direct-drive wind turbine grid interfacing. *IEEE Trans. Ind. Electron.* **2013**, *60*, 509–522.
4. Ruba, M.; Szabo, L.; Jurca, F. Fault Tolerant Switched Reluctance Machine for Wind Turbine Blade Pitch Control. In Proceedings of the 2009 International Conference on Clean Electrical Power, Capri, Italy, 9–11 June 2009; pp. 721–726.

5. Cuzzola, F.A.; Morari, M. A Generalized Approach for Analysis and Control of Discrete-Time Piecewise Affine and Hybrid Systems. In *Hybrid Systems: Computation and Control Lecture Notes in Computer Sciences*; Springer: Berlin/Heidelberg, Germany, 2001; pp.189–203.
6. Johansson, M.; Rantzer, A. Computation of piecewise quadratic Lyapunov functions for hybrid systems. *IEEE Trans. Autom. Control* **1998**, *43*, 555–559.
7. Rantzer, A. Piecewise linear quadratic optimal control. *IEEE Trans. Autom. Control* **2000**, *45*, 629–637.
8. Hassibi, A.; Boyd, S. Quadratic Stabilization and Control of Piecewise-Linear Systems. In Proceedings of the American Control Conference, Philadelphia, PA, USA, 21–26 June 1998; pp. 3659–3664.
9. Pettersson, S.; Lennartson, B. LMI for Stability and Robustness of Hybrid Systems. In Proceedings of the American Control Conference, Albuquerque, NM, USA, 4–6 June 1997; pp. 1714–1718.
10. Slupphaug, O.; Foss, B.A. Constrained quadratic stabilization of discrete time uncertain nonlinear multi-model systems using piecewise affine state feedback. *Int. J. Control* **1999**, *72*, 686–701.
11. Mignone, D.; Ferrari-Trecate, G.; Morari, M. Stability and Stabilization of Piecewise Affine and Hybrid Systems: An LMI Approach. In Proceedings of the 39th IEEE Conference on Decision and Control, Sydney, Australia, 12–15 December 2000; pp. 504–510.
12. Gang, F. Stability analysis of piecewise discrete-time linear systems. *IEEE Trans. Autom. Control* **2002**, *47*, 1108–1112.
13. Esbensen, T.; Sloth, C. *Fault Diagnosis and Fault-Tolerant Control of Wind Turbine*; Aalborg University: Aalborg, Denmark, 2009.
14. Højstrup, J. Velocity spectra in the unstable planetary boundary layer. *J. Atmos. Sci*. **1982**, *39*, 2239–2248.
15. Thomsen, S. *Nonlinear Control of a Wind Turbine*; Technical University of Denmark: Kgs. Lyngby Copenhagen, Denmark, 2006.
16. Østergaard, K.Z.; Brath, P.; Stoustrup, J. Estimation of effective wind speed. *J. Phys.* **2007**, *75*, 1–9.
17. Burkart, R.M.; Margellos, K.; Lygeros, J. Nonlinear Control of Wind Turbines: An Approach Based on Switched Linear Systems and Feedback Linearization. In Proceedings of the 50th IEEE Conference on Decision and Control and European Control Conference, Orlando, FL, USA, 12–15 December 2011; pp. 5485–5490.
18. Odgaard, P.F.; Aalborg, U.; Stoustrup, J.; Kinnaert, M. Fault-tolerant control of wind turbines: A benchmark model. *IEEE Trans. Control Syst. Technol*. **2013**, *21*, 1168–1182.
19. Sloth, C.; Esbensen, T.; Stoustrup, J. Robust and fault-tolerant linear parameter-varying control of wind turbines. *Mechatronics* **2011**, *21*, 645–659.
20. Rotondo, D.; Nejjari, F.; Puig, V.; Blesa, J. Fault Tolerant Control of the Wind Turbine Benchmark Using Virtual Sensors/Actuators. In Proceedings of the 8th IFAC Symposium on Fault Detection, Supervision and Safety of Technical Processes, National Autonomous University of Mexico, Mexico, 29–31 August 2012; pp.114–119.
21. Zhang, H.B.; Dang, C.H.; Zhang, J. H_∞ control of piecewise-linear systems under unreliable communication links. *Circuits Syst. Sign. Process*. **2012**, *31*, 1297–1318.

22. Munteanu, I.; Cutululis, N.-A.; Bratcu, A.L.; CeangĂ, E. *Optimal Control of Wind Energy Systems*; Springer: London, UK, 2008.
23. Zhang, H.; Shi, Y. Observer-based H_∞ feedback control for time-varying discrete-time systems with intermittent measurements and input constraints. *ASME J. Dyn. Syst. Meas. Control.* **2012**, *134*, doi:10.1115/1.4006070.
24. Shi, Y.; Huang, J.; Yu, B. Robust tracking control of networked control systems: Application to a networked DC motor. *IEEE Trans. Ind. Electron.* **2013**, *60*, 5864–5874.